

Wiebke Breves · Rüdiger Heuermann · Rainer Reuter

## Enhanced red fluorescence emission in the oxygen minimum zone of the Arabian Sea

Received: 22 May 2002 / Accepted: 18 February 2003  
© Springer-Verlag 2003

**Abstract** Depth profiles of fluorescence at several excitation and emission wavelengths were measured along with CTD data during the cruise So119 of RV *Sonne* in the Arabian Sea from 12 May to 10 June 1997. In addition to chlorophyll fluorescence from phytoplankton in the near-surface layer, the profiles in the oxygen minimum region well below the euphotic zone show enhanced red fluorescence. Red fluorescence intensity is inversely related to the oxygen concentration in intermediate and deep waters. A relationship to characteristic water masses of the region cannot be found in the data, and this holds also with chemical data such as DOC. Absorbance spectra of water samples taken in the oxygen minimum zone show an absorption band at 420 nm wavelength with about 50 nm bandwidth, much weaker than gelbstoff absorbance in the same wavelength range. The absorption band remains stable after sample filtration with 0.45  $\mu\text{m}$  glass fibre filters. Hence, the size of the absorbing matter is in the range of dissolved molecules or particles much smaller than 1  $\mu\text{m}$ . Fluorescence spectra of unfiltered samples with 420 nm excitation show a weak emission band at 600 nm and a more pronounced one at 660 nm wavelength. The trailing edge of the 660 nm band falls into the range of chlorophyll emission, thus giving rise to the observed depth profiles of red fluorescence in the oxygen minimum zone. Red fluorescence measured on samples remain stable during a few hours after sampling even in the presence of oxygen. It is not detectable after several weeks of sample storage in the dark and cannot be reproduced even after depletion of dissolved oxygen.

**Keywords** Fluorescence · Red fluorescence · DOM · Gelbstoff · Oxygen minimum zone · Arabian Sea · Chlorophyll

### 1 Introduction

Since the beginning of fluorescence measurements in oceanography (Kalle 1963), the use of fluorescence to detect gelbstoff and phytoplankton pigments by their specific fluorescence characteristics has been well developed. Today, such measurements on water samples or with in situ sensors are widely used to identify water masses and to quantify biomass and primary production (Yentsch and Menzel 1963; Lorenzen 1966; Chen and Bada 1992; Coble 1996; and many others).

When excited at 420 nm, fluorescence emission at 680 nm is thought to originate from phytoplankton chlorophyll *a* and phaeopigments. Such signals are typically found in the upper photic layers of the water column, depending on the presence of phytoplankton biomass.

Gelbstoff (yellow substance) is the light-absorbing part of dissolved organic matter (DOM) in water. Due to its fluorescence it can be specifically and sensitively detected. When excited in the near-ultraviolet it fluoresces over a wide spectral range at blue–green wavelengths. The emission maximum is at 420 to 450 nm, depending on its origin (De Souza Sierra and Donard 1991; Coble 1996). The use of 420 nm as excitation wavelength results in gelbstoff fluorescence signals with a maximum at about 500 nm. Intensities at emission wavelengths above 620 nm are marginal compared with the emission at blue–green wavelengths and can be neglected in oceanic waters where gelbstoff concentrations are low.

On a cruise in the Arabian Sea fluorescence measurements were carried out in situ and in vitro in addition to CTD and oxygen depth casts. The analyses of biological and chemical parameters on water samples such as phytoplankton chlorophyll *a*, DOC, O<sub>2</sub> and

Responsible Editor: Andreas Oschlies

W. Breves · R. Heuermann · R. Reuter (✉)  
Carl von Ossietzky Universität Oldenburg,  
Fachbereich Physik, 26111 Oldenburg, Germany  
e-mail: rainer.reuter@uni-oldenburg.de

R. Heuermann  
TriOS Optical Sensors GmbH,  
26111 Oldenburg, Germany

others were done by the Institute of Biogeochemistry and Marine Chemistry of the University of Hamburg. The JGOFS cruise So119 of RV *Sonne* took place from 12 May to 10 June 1997 during the onset of the south-west monsoon. Positions of stations were selected in the more oligotrophic central Arabian Sea as well as in the upwelling region near the Omani coast (Fig. 1). The hydrography of this region is well described in the literature, (see, for example, Shetye et al. 1994 and references given therein).

Dissolved oxygen in the Arabian Sea shows a distinct minimum between 200 and 1000 m depth where the concentrations are close to zero. Suboxic conditions are generally produced by intense oxygen sinks caused by the large input of organic matter, and/or by the distance in time from sources of oxygen renewal such as the sea surface. Estimates of oxygen consumption and mean annual surface production are within the broad range of oligotrophic regions (Warren 1994) and cannot explain the low oxygen levels in the oxygen minimum zone (OMZ) of the Arabian Sea. The most likely reason seems to be the inflow of already oxygen-depleted water (Warren 1994). The rates of new production and the export of organic matter into deeper layers sustain the presence of an almost complete oxygen depletion (Lal 1994).

Depth profiles of fluorescence measured during So119 with 420 nm excitation and 680 nm emission wavelength, aiming at a detection of phytoplankton chlorophyll *a* via its specific fluorescence, reveal signals in the OMZ with intensities comparable to those from phytoplankton in the near-surface layer. In a first approximation this fluorescence is inversely correlated with the profile of the oxygen concentration in the intermediate and deep-water layer.

Red fluorescence at depths well below the euphotic zone was first reported by Anderson (1982) for the Pacific Ocean. It was described in more detail by Broenkow

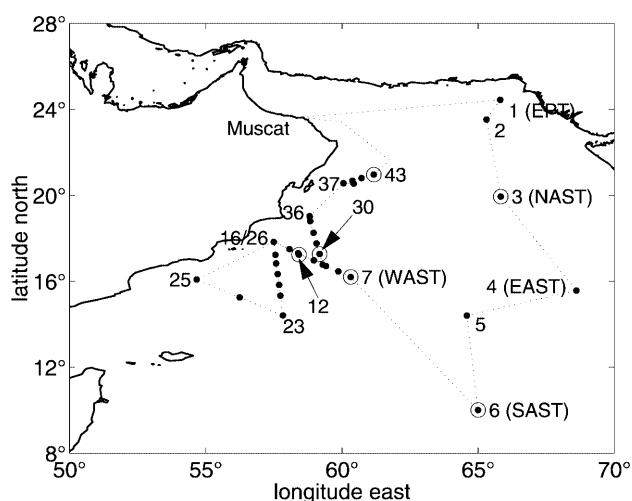


**Fig. 1** Cruise track and position of stations of the cruise So119 of RV *Sonne* in the Arabian Sea, 12 May to 10 June 1997. Circled positions refer to locations where measured depth profiles are shown in figures below

et al. (1983, 1985) for the eastern tropical and the central North Pacific Ocean. Using an in situ chlorophyll fluorometer in aphotic depths they found one to two layers with significant chlorophyll-like fluorescence signals, denoted as secondary and tertiary maxima. We report here for the first time similar but much more pronounced features in the Arabian Sea. The objective of this paper is to present these data and to relate these fluorophores to physical, biological and chemical conditions in the Arabian Sea.

## 2 Methods

### 2.1 Sampling

Water samples were taken using a rosette with 24 10.1 Niskin bottles assembled to a Seabird 911+ CTD probe. Sampling was mostly done at depths corresponding to 5-35-50-80-120-150-200-300-450-600-800-1000-1250-1500-2000-2500-3000-3500 and 4000 m. The samples collected for in vitro fluorescence and absorbance measurements were filled into amber 500 ml glass bottles and stored in isolating boxes to keep the samples at their in situ temperature. Optical measurements were mostly done immediately after sampling and completed about 3 h later. DOC and phytoplankton chlorophyll data were taken by the Institute of Biogeochemistry and Marine Chemistry of the University of Hamburg.

### 2.2 In vitro optical measurements

Fluorescence measurements on samples were made with a Perkin Elmer model LS50 luminescence spectrometer with 420 nm excitation wavelength over an emission wavelength range of 450 to 750 nm. This procedure is described in detail in Breves and Reuter (2000). Absorbance measurements were made from 200 to 800 nm wavelength with a Perkin Elmer model Lambda 18 spectrophotometer using two fused silica cuvettes of 10 cm pathlength in the sample and the reference light path of the instrument. Each sample was measured in untreated form and after filtration on a Schleicher & Schüll GF 50 glass fibre filter with 0.45  $\mu\text{m}$  pore size against purified water in the reference cuvette. The filters were pre-combusted at 450  $^{\circ}\text{C}$  for 5 h to avoid sample degradation from organic impurities in the filter material. The resolution of the calculated absorption coefficient is  $\Delta a = 0.002 \text{ m}^{-1}$ ; the maximum error due to electronic drift is estimated to be  $0.03 \text{ m}^{-1}$ .

For further investigations, samples taken in the OMZ were stored at 4  $^{\circ}\text{C}$  temperature in amber glass bottles and with minimum residual air volume inside the bottles. One year after the cruise, their absorbance and fluorescence properties were again investigated. The samples were then treated with argon gas to achieve oxygen depletion over a period of 3 months, and further optically analyzed during that time.

### 2.3 In situ measurements

A bio-optical sensor package was used which includes a CTD probe (model OTS 3000, ME Meerestechnik Elektronik, Germany) with a Clark-type oxygen sensor, and a fluorometer with 270 and 420 nm excitation wavelengths (Barth et al. 1997). The maximum operating depth of the sensor package is 3000 m. The fluorescence data presented in this paper were obtained with the following combinations of excitation and emission (ex/em) wavelengths in nanometres: (270/450) for gelbstoff, (420/680) for chlorophyll fluorescence measurements and (270/300) for measuring water Raman scatter, which is used for normalizing the fluorescence readings of other detection modules (Heuermann et al. 1995). Raman scatter was measured with 10 nm bandwidth on both the excitation and the emission sides. The bandwidth for 450 nm gelbstoff and 680 nm chlorophyll measurements was 20 nm. The precision of the depth profiles measured with in situ fluorometer is high, as can be seen in repeated casts made at the same location (Fig. 2).

## 3 Results

### 3.1 In situ fluorescence and oxygen

Depth profiles of red (420/680) fluorescence measured during the So119 cruise show two characteristic features (Figs. 3, 4). The first and expected one is a signal in the near-surface layer down to about 100 m depth. This is related to chlorophyll fluorescence of phytoplankton in

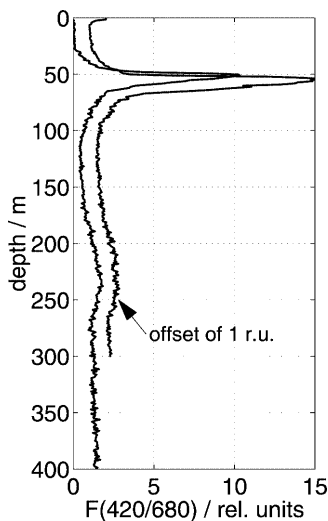


**Fig. 2** Results of repeated in situ profiling of fluorescence with 420 nm excitation and 680 nm emission wavelength at identical locations at station 7, cast 2 (*left*) and cast 8 (*right*) with a time lapse of 13.5 h. An additional offset of 1 relative unit is added to the data from cast 8 for better visualization. Reproducibility of the profiles is high, except for the chlorophyll *a* fluorescence maximum at about 50 to 100 m depth, which is variable due to phytoplankton patchiness

the euphotic zone. Extracted chlorophyll *a* concentrations in the upper 150 m are below  $1 \mu\text{g l}^{-1}$ ; values from greater depths are not available. The second feature is a steep increase in the intensity at depths below the euphotic zone. It attains a flat maximum at about 200 to

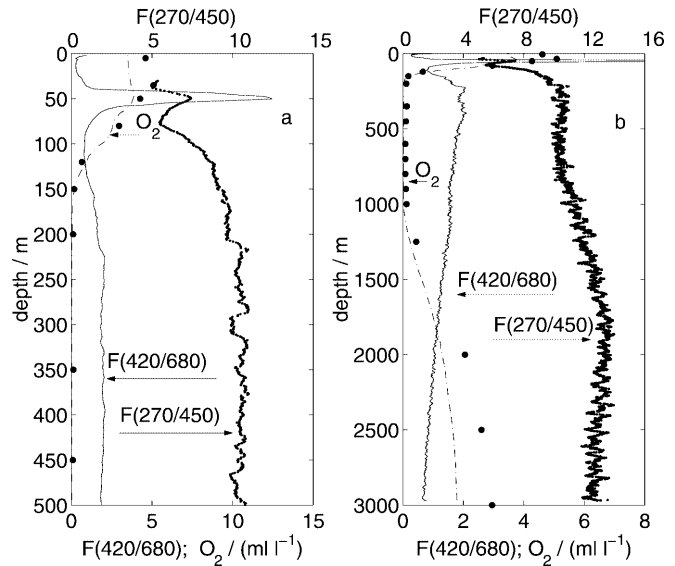


**Fig. 3a, b** Depth profile of red F(420/680) and gelbstoff F(270/450) fluorescence and dissolved oxygen (*dots* Winkler method; *dashed-dotted line* in situ) at station 3 (NAST), 16 May 1997. The in situ fluorescence data is smoothed (moving average over 11 m, F(270/450) is given in  $10^{-3}$  Raman units  $\text{nm}^{-1}$ , F(420/680) in relative units). **a** 0–500 m, **b** 0–3000 m, the *upper horizontal axis* belongs to gelbstoff, the *lower axis* to the red fluorescence and dissolved oxygen concentration. The surface gelbstoff fluorescence measurement was degraded by sunlight and is therefore excluded. The in situ oxygen measurement systematically underestimates the oxygen concentration, but its qualitative dynamics are consistent with the data measured by the Winkler method

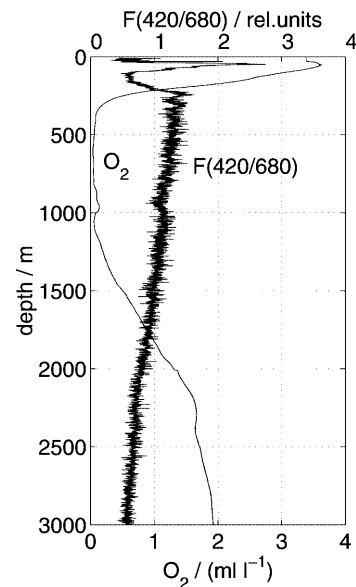


**Fig. 4** Depth profile of red F(420/680) fluorescence and dissolved oxygen at station 30, position  $17^{\circ}16\text{N}$ ,  $59^{\circ}11\text{E}$ , 1 June 1997

300 m depth, mostly followed by a monotonic decrease in the intermediate layer and down to deep waters. Its intensity reaches levels that are mostly of the same order of magnitude as the near-surface chlorophyll fluorescence, and up to half the value at the chlorophyll maximum. It is thus far from a marginal effect.

Of particular interest is the distribution of dissolved oxygen. A number of these profiles are given in the appendix. Oxygen concentrations of about 4 to 5 ml l<sup>-1</sup> in the near-surface layer decrease to less than 0.1 ml l<sup>-1</sup> at 200 m depth and in the entire intermediate layer which forms the oxygen minimum zone (OMZ) of the Arabian Sea. At depths of more than 1000 m the concentration increases again monotonically, reaching values of about 3 ml l<sup>-1</sup> at 3000 m depth (Fig. 3). Except for the near-surface water where phytoplankton is found, the red fluorescence profile shows an inverse trend when compared with the oxygen profile. This covariance holds even down to the scales of small-scale features that were observed at some of the stations (Fig. 4). The actual gradient of both entities might differ, however; e.g., while the enhanced red fluorescence decreases more or less monotonically from 200 to 3000 m, the oxygen profiles show a flat minimum in the OMZ and increasing values below 1000 m.

Examples of profiles of the (270/450) gelbstoff fluorescence are also shown in Fig. 3. A relation to the red (420/680) fluorescence profile, as observed with oxygen, is only apparent at the top of the OMZ (100...500 m), where both signals show strong gradients. Gelbstoff profiles are generally characterized by low values in the mixed layer, as a result of sunlight-induced photodegradation (Moran and Zepp 1997, and references cited therein). At the depth of the chlorophyll fluorescence peak a similar gelbstoff fluorescence peak is found due to phytoplankton and the release of fluorescent exudates. In the intermediate and deep water the gelbstoff signal is higher and more homogeneous than in the upper water column. At intermediate depths where dissolved oxygen values are close to zero the signal is smaller than in deep waters.

### 3.2 Physical parameters and red fluorescence

The profiles of potential temperature  $\Theta$  and salinity  $S$  were used to plot  $\Theta S$ -diagrams for an identification of characteristic water masses. Data from stations 3 (NAST), 6 (SAST), 12 and 43 are shown in Fig. 5 as typical examples to illustrate the distribution of water masses in the northern and southern Arabian Sea and off the Omani coast (Fig. 1). The presence of Arabian Sea High Salinity Water (ASHSW) in the upper water column and North Indian Deep Water (NIDW) in deep waters is obvious. In the northern Arabian Sea, Persian Gulf Water (PGW) is found in the upper water column (see stations 3 and 43 at about 250...350 m depth). Red Sea Water (RSW) is present in the south at intermediate depths in variable quantities (see station 6) and is less pronounced than PGW.

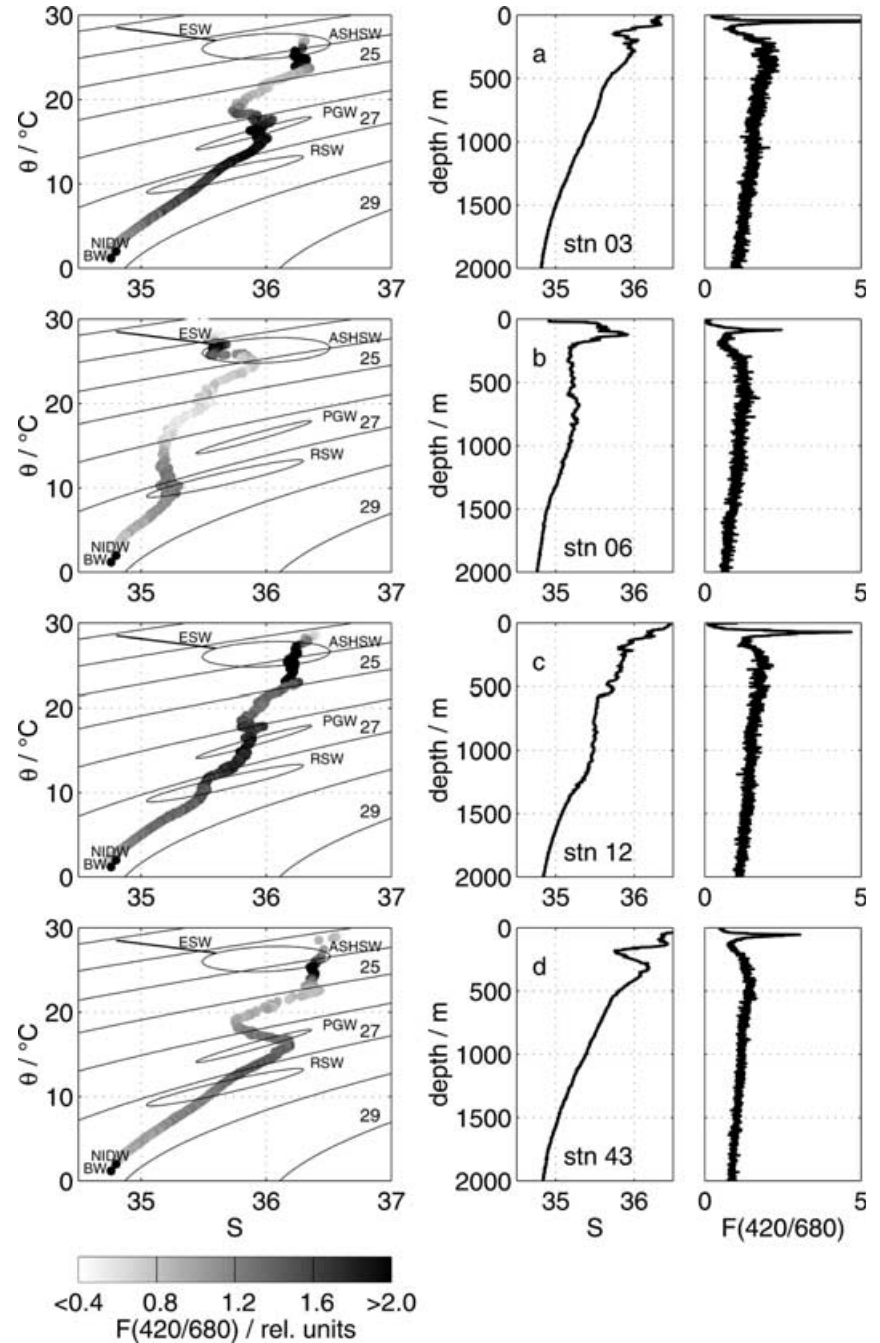
Attempts were made to relate the intensity of red fluorescence below the euphotic layer to these water masses, which would help to understand the origin of this signal. The water masses PGW and RSW at the lower end of the upper water column and at intermediate depths are possible candidates. For this, the  $\Theta/S$  profiles in Fig. 5 are shown with grey levels that indicate the red fluorescence intensity. Again, near-surface chlorophyll  $a$  fluorescence peak and the deep red fluorescence are well-defined structures in these diagrams. However, the strong fluorescence signal in the PGW water at station 3 is much less dominant in the same water mass at station 43. Much weaker quantities of PGW are found at station 12, but red fluorescence is high. At station 6 the intermediate RSW coincides with slightly higher signals, but the lower portions of RSW at the other stations do not show a similar enhanced signal. In conclusion, a direct relation of red fluorescence to characteristic water masses of the Arabian Sea cannot be stated. This optical property is not restricted to small subregions, but advective transport via one of the dominant water masses of the Arabian Sea seems very unlikely.

### 3.3 In vitro fluorescence, DOC and oxygen

Emission spectra taken on samples with 420 nm excitation are useful to investigate the spectral characteristics in more detail (Fig. 6). The sample from 35 m depth is characterized by low gelbstoff fluorescence due to photodegradation, and by chlorophyll fluorescence from phytoplankton. Samples from greater depths show an almost identical but stronger gelbstoff signal at blue-green wavelengths. Both samples taken in the OMZ, e.g., at 450 and 1000 m depth, show two other fluorescence bands centred at 600 and 660 nm. Their intensity is comparable to the chlorophyll signal from the near-surface sample. In the 3000 m sample taken well below the OMZ, these signals are almost absent, and a continuous decrease of the 500 nm fluorescence peak towards the red part of the spectrum up to 700 nm is found.

Fluorescence emission signals at 530, 600, 660 and 680 nm with 420 nm excitation were extracted from all measured spectra for further analysis. Depth profiles derived in this way are shown in Fig. 7 for the same station as in Fig. 3. The signal intensities of the (420/530) profile display the expected distribution of gelbstoff fluorescence at these excitation and emission wavelengths. The (420/600) signals show an increase in the OMZ and a broad maximum at approximately 500 to 1200 m depth. The 660 and 680 nm profiles are similar, but intersect at approximately 120 m. In the upper 120 m the leading edge of the 680 nm chlorophyll  $a$  emission band accounts for the weak signal at 660 nm. At depths of more than 120 m it is the emission band centred at 660 nm with its trailing edge extending well into the region of the 680 nm fluorescence which causes the alleged chlorophyll-like fluorescence there.

**Fig. 5**  $\Theta$ - $S$ -diagrams (*left*) and profiles of salinity  $S$  and  $F(420/680)$  fluorescence (*right*) at four stations that are representative of the investigated area. **a–d** **a** Station 3 (NAST), 16 May 1997 **b** Station 6 (SAST), 21 May 1997 **c** Station 12, 26 May 1997 **d** Station 43, 5 June 1997. *Solid lines* in the  $\Theta$ - $S$ -diagrams are contours of potential density. The characteristics of ASHSW, PGW, RSW, NIDW and Bottom Water (BW) are indicated (Shetye et al. 1994), see text for abbreviations of water masses. The  $\Theta$ - $S$ -diagrams are grey-coded to display the intensity of in situ red  $F(420/680)$  fluorescence



The shape of DOC profiles varies over the sample area. Figure 8 shows as typical examples the profiles from stations 3 (NAST) and 7 (WAST) down to 500 m depth together with the in vitro (420/660) fluorescence, and the chlorophyll  $a$  concentration measured in the upper 150 m. Except for a few data points, DOC values in the euphotic zone are slightly higher than at larger depth. There is no apparent relationship between DOC and the (420/660) fluorescence profile. Hence, there are no indications of a specific change of DOC, which might be connected with the increased red fluorescence there.

The relationship of in vitro fluorescence versus dissolved oxygen (Winkler method) is presented in Fig. 9a–d. Here, only samples taken at depths greater than 200 m were considered to eliminate the influence of “real” chlorophyll  $a$  fluorescence in the euphotic zone of the water column. No correlation was found for gelbstoff (420/530 and 420/600), while emission at 660 and 680 nm exhibited a slight decrease with oxygen. The squared Pearson correlation coefficient of  $r^2 = 0.8$  (Fig. 9) probably results from the highly scattered signals at low oxygen levels.

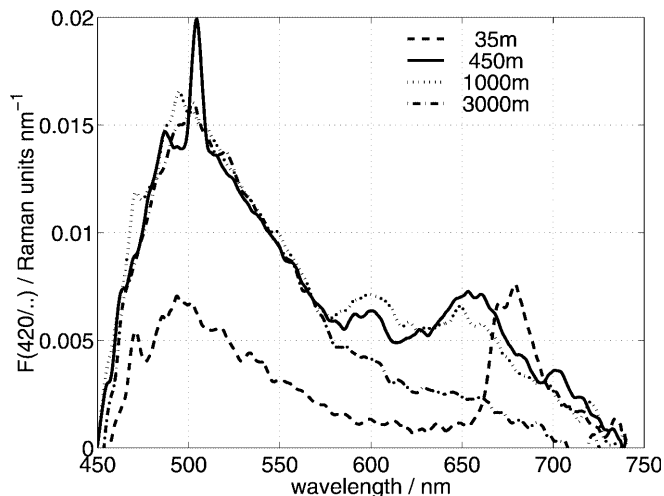


**Fig. 6** Emission spectra from samples taken at station 3 (NAST), position 19°57N, 65°50E, 16 May 1997 (see Fig. 3 for comparison) from 35, 450, 1000 and 3000 m depth. Excitation wavelength is 420 nm. Water Raman scattering at 490 nm is not visible due to the subtraction of the blank spectra of purified water, as described in the section 2.3. Spectra are smoothed with a moving average over 5 nm

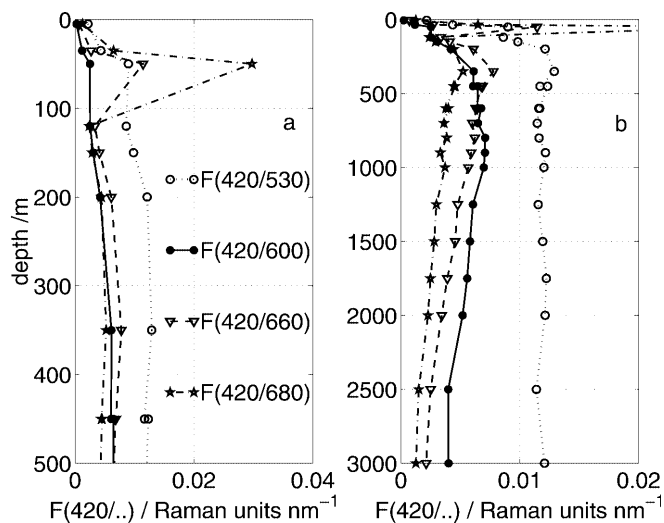


**Fig. 7a, b** Fluorescence depth profiles at station 3 (NAST), derived from measurements on water samples with 420 nm excitation and emission wavelengths as given in the figure. Emission signals are averaged over  $\pm 10$  nm to reduce the noise in the spectra

### 3.4 In vitro absorbance

More information can be found from a closer view of the spectra of the absorption coefficient  $a$  measured with the laboratory spectrophotometer. All spectra show the typical exponential decrease from the ultraviolet to the red part of the spectrum that is due to gelbstoff. However, in samples taken in the oxygen minimum zone there is an additional absorption band centred at 420 nm (Fig. 10). It is not affected by sample filtration with Schleicher & Schüll GF 50 0.45  $\mu\text{m}$  glass fibre fil-

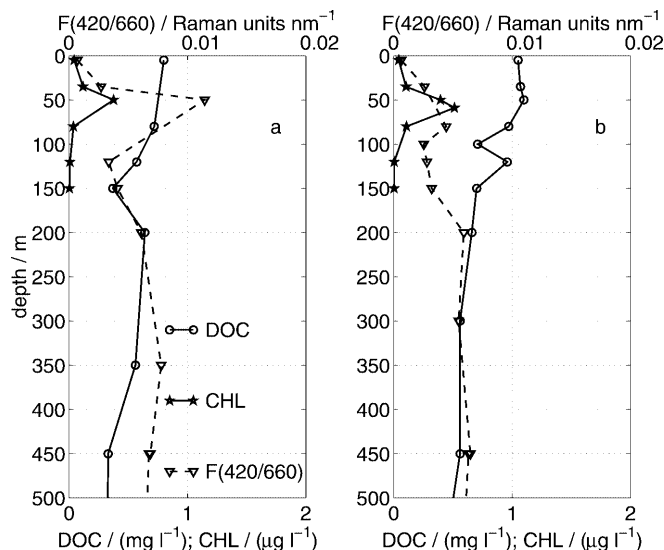


**Fig. 8a, b** DOC, F(420/660) fluorescence and extracted chlorophyll profiles: **a** at station 3 (NAST) and **b** at station 7 (WAST)

ters. The material causing this absorption band is thus smaller than about 0.45  $\mu\text{m}$ . It would therefore belong to the dissolved fraction, according to the practical definition of dissolved and particulate matter.

The excitation wavelength of both the in situ and in vitro fluorescence measurements is identical with the spectral position of this absorption band. Hence, it is most likely that the observed red fluorescence is connected to material showing this absorption band. The spectra were analyzed in the wavelength range of 350 to 650 nm with the least-squares fit of  $a_1$ ,  $S$ ,  $a_2$  and  $a_3$  in

$$a(\lambda) = a_1 e^{-S(\lambda-\lambda_0)} + a_2 \frac{1}{\sqrt{2\pi}\sigma} e^{-\frac{-(\lambda-\lambda_0)^2}{2\sigma^2}} + a_3.$$

The first term on the right side corresponds to the exponential characteristic of the gelbstoff absorption coefficient as it is typically found in seawater. The exponential slope  $S$  ranges between 0.013 and 0.023  $\text{nm}^{-1}$  (Breves and Reuter 2000), which is higher than the mostly typical value of 0.014  $\text{nm}^{-1}$  (Bricaud et al. 1981). The second term is a Gaussian function which is used to describe the absorption band, with peak wavelength and standard deviation set to  $\lambda_0 = 420$  nm and  $\sigma = 30$  nm. The third term,  $a_3$ , describes a possible offset in the spectra due to electronic drift.

The vertical distribution of the amplitude factor  $a_2$  of the Gaussian part of the fit is shown in Fig. 11a for filtered and original samples from station 7 (WAST). Obviously, sample filtration does not affect the  $a_2$  profile. Its shape coincides with the profile of the red fluorescence, except for the near-surface chlorophyll  $a$  fluorescence, where  $a_2$  is zero (Fig. 11b). Figure 12 shows the high correlation of  $a_2$  and the (420/680) fluorescence signal, again calculated with sample data from depths of more than 200 m.

**Fig. 9** Correlation plots of fluorescence on samples with the laboratory luminescence spectrometer and dissolved oxygen (Winkler method). From left to right F(420/530), F(420/600), F(420/660) and F(420/680). Fluorescence is given in Raman units  $\text{nm}^{-1}$ . Only data from depths of more than 200 m were considered to exclude “real” chlorophyll *a* fluorescence

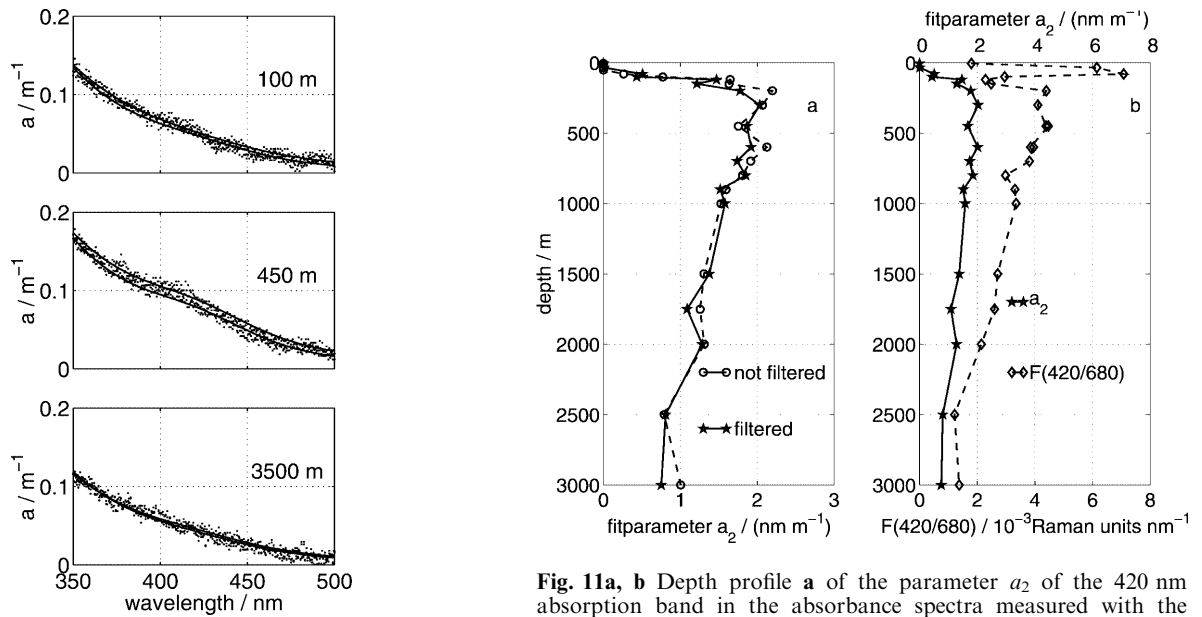
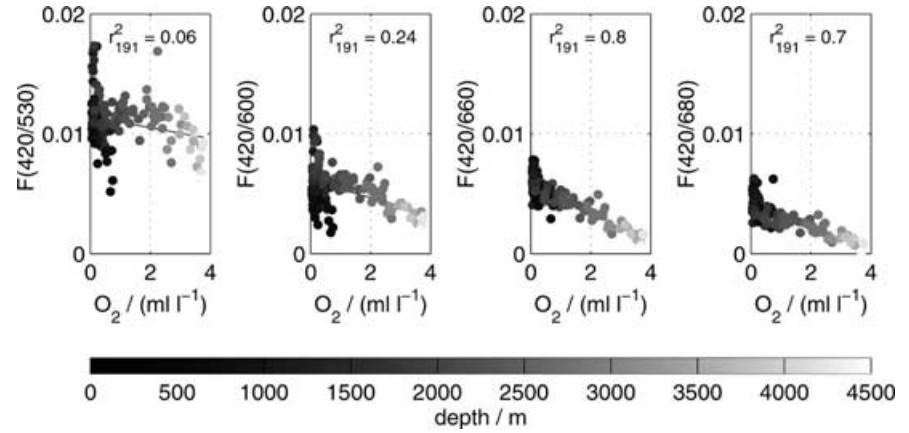


**Fig. 10** Spectra of the absorption coefficient of original and filtered water samples taken at station 7 (WAST), position  $16^{\circ}12\text{N}$ ,  $60^{\circ}19\text{E}$ , 24 May 1997, from 100, 450 and 3500 m depth. Spectra are corrected for small electronic offset contributions. Thin lines correspond to a fit in the 350 to 650 nm wavelength range, as described in the text

## 4 Discussion

### 4.1 Water masses

Naqvi (1991) suggests a formation of lower-salinity water near the coast of Gujarat and the Gulf of Kutch, which advects into the OMZ, accounting for the salinity minimum at about 200 m. This might inject appreciable quantities of DOC. The salinity minimum, discussed in detail by Shenoi et al. (1993), is clearly visible in our data. However, it cannot be related to the red fluorescence, since it is also present where an intense salinity minimum is not found.

In the literature, opinions vary about the dominating water types/masses, which mix in the Arabian Sea. You

**Fig. 11a, b** Depth profile **a** of the parameter  $a_2$  of the 420 nm absorption band in the absorbance spectra measured with the laboratory spectrophotometer on water samples from unfiltered and filtered samples at station 7 (WAST); **b** of the F(420/680) fluorescence and the parameter  $a_2$  of the filtered sample. The parameter  $a_2$  on the abscissa is the amplitude factor of a Gaussian function used as a fit of the absorption band. See text for further explanations

and Tomczak (1993) report on three main water masses, that is Indian Central Water (ICW), Australasian Mediterranean Water (AAMW) and Red Sea Water (RSW) that contribute to the mixing of the thermocline, while the influence of Persian Gulf Water (PGW) is stated to be small. Shetye et al. (1994) found that the characteristics of the upper 1000 m are a mix of ASHSW, RSW, PGW and Indian Ocean Equatorial Water (IEW). Referring to You and Tomczak (1993) the IEW is a mixture of ICW and AAMW. Kumar et al. (1990), on the other hand, include ASHSW, PGW, RSW, North Indian Ocean Bottom Water and Antarctic Bottom Water in their list of water masses of the Arabian Sea.

In the CTD data of So119 and following the classification of Shetye et al. (1994) the ASHSW and NIDW water masses could be identified in all depth profiles.

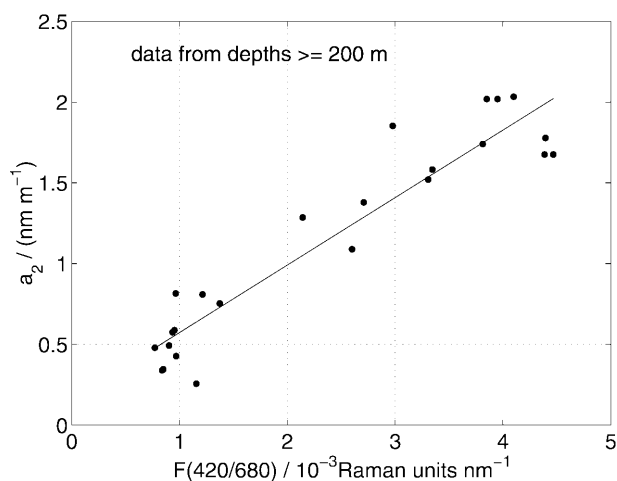


**Fig. 12** Correlation plot between fluorescence and  $a_2$  values at station 7 (WAST) (see Fig. 11 and explanation given there). The correlation coefficient is  $r^2 = 0.89$

PGW and RSW water were also present in varying quantities, depending on the investigated region, the PGW being a dominant feature in the upper water column north of  $18^\circ\text{N}$ . The detailed analysis of the depth profiles of temperature, salinity and red fluorescence taking into account this water mass classification leads to the result that the inflow and mixing of PGW and RSW does not explain the observed red fluorescence. Despite the variations in the red fluorescence there is no clear relationship to water masses, and the same holds for the spatial distribution of DOC and chlorophyll in the Arabian Sea.

#### 4.2 Oxygen

The squared Pearson correlation coefficient  $r^2 = 0.8$  of the (420/660) fluorescence versus dissolved oxygen concentrations below the euphotic zone and down to deep waters indicates the potential importance of oxygen deficiency. It cannot explain whether it is a chemical long-term reaction or rather a biologically triggered effect that occurs in oxygen-deficient waters, caused by a bacterial population and its potential interaction with detritus. A fluorometric and photometric analysis of water samples from the oxygen minimum zone about 1 year following the cruise showed neither red fluorescence or an absorption band at 420 nm wavelength. These features could not be regenerated by treating samples with argon gas to achieve oxygen depletion over a period of 3 months. Hence, red fluorescence emission cannot be generated under laboratory conditions. Possible reasons might be the changed oxygen content during the storage period, alteration and degradation of dissolved fluorescent substances, or changes in bacterial populations and activities. On the other hand, both the red fluorescence and the 420 nm absorption band remained stable within a period of

hours required for the on-board sample analysis during the cruise. Hence, the fluorophore is not rapidly degraded by the occurrence of oxygen.

#### 4.3 Absorption spectra

In the context of the description of deep red fluorescence, the examination of absorption spectra is a new aspect. As can be seen in Figs. 11 and 12, the absorption band centred at 420 nm within the OMZ is a striking feature. The levels of (420/660) fluorescence and 420 nm absorbance are well correlated (Fig. 12). Apparently, red fluorescence can only be observed with a choice of the excitation wavelength within this absorption band. It is not yet known if the orange (420/600) fluorescence (Fig. 6) is connected to the same absorption band as well. Its closer inspection is difficult, because it is weaker and interferes with the trailing edge of gelbstoff fluorescence.

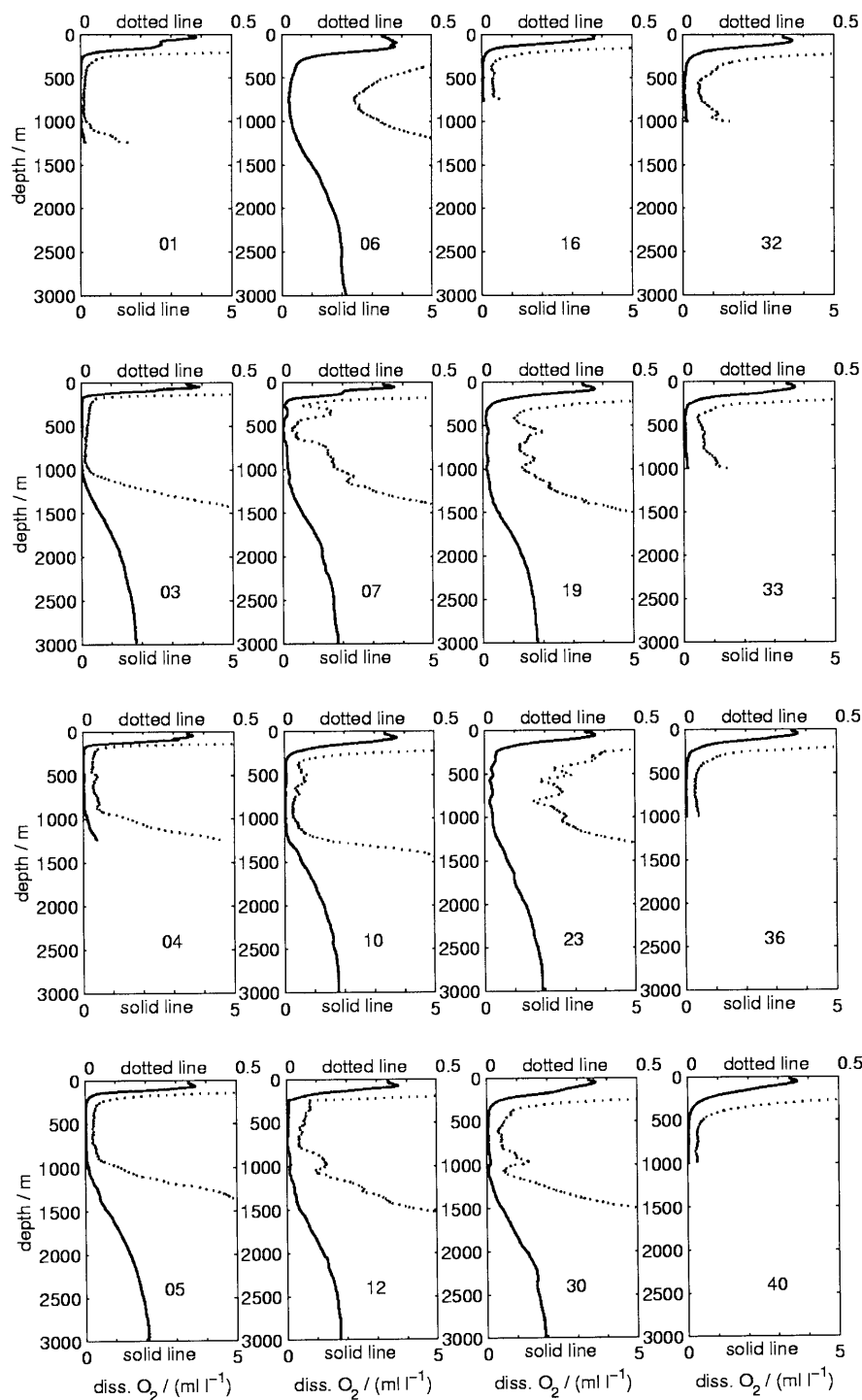
The comparison of spectra from original and filtered samples showed no significant differences. Red fluorescence and the 420 nm absorption band are related to the dissolved fraction. This would contradict Broenkow et al's (1992) hypotheses of a particular origin. Bacteria and picoplankton, however, pass through filters with  $0.45 \mu\text{m}$  pore size and are therefore still candidates for fluorophores. The spectral signature of their pigments may be superimposed on a detrital-type absorption (Nelson 1993), thus being only weakly detectable in absorption spectra. Nelson showed that the spectral absorption of phytodetritus can be altered in the presence of active-growing bacterial populations. His findings and the conclusions of Naqvi (1994) still sustain the possibility that the observed changes in absorption spectra may be due to bacterial populations.

#### 4.4 Turbidity layers in the Arabian Sea

Measurements of nitrite, particulate protein, bacterial abundance and the beam attenuation (Naqvi et al. 1993; Naqvi 1994) show a turbid layer at intermediate depths of the Arabian Sea which does not seem to be restricted to any special water masses. It rather depicts a correlation to the broad secondary nitrite maximum of the Arabian Sea. Intense denitrification there leads to maximum nitrite concentrations as intermediates of the denitrification. The particle maximum might be associated with a probably large living organic content and led to the suggestion that bacteria directly cause the increased beam attenuation at these depths.

Qasim (1982) calculated nitrate deficits for different depths of the northern Arabian Sea and constructed a nitrate anomaly curve, indicating that nitrate reduction takes place over a depth range from about 70 to 1750 with a maximum at 300 m, a depth where also a substantial diel vertical migration (DVM) of mesozooplankton takes place (Wishner et al. 1998). Their biomass depth profiles showed close relationships to oxygen. The contribution

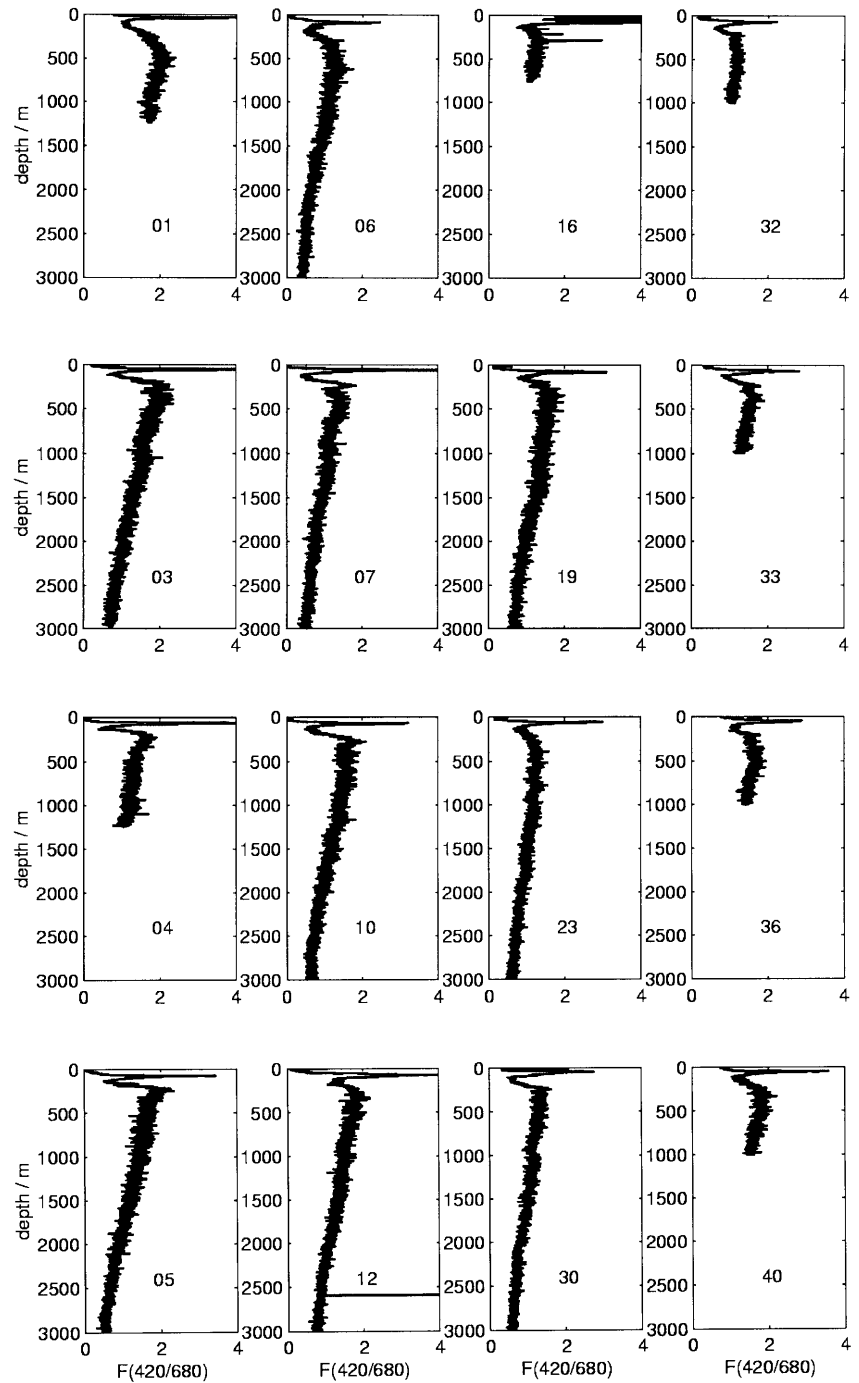
**Appendix 1** Profiles of dissolved oxygen from selected stations. The chosen stations cover main (trap) stations and representative stations from transects and depict the variability found in the sampled area. To show off small-scale variations in the suboxic regions, an additional zoom of the dissolved oxygen profile is drawn (dotted lines and upper axis)



and modification of the vertical flux of material to depth due to the zooplankton feeding behaviour in surface waters and the excretion, defaecation or respiration at depth possibly leads to the intermediate nepheloid layer occurring from 150 to 300 m. They provide a source of nutrients and a substrate for bacteria (Wishner et al. 1998, and references therein). Thus, nitrate reducers and zooplankton play an active part in the biogeochemistry in this depth range, being potential contributors for the occurrence of red fluorescence.

On a previous RV *Meteor* cruise in 1995 (M32/5) and a succeeding RV *Sonne* cruise from 12 June to 12 July 1997 (So120), total bacterial numbers and total bacterial biomass were determined in the Arabian Sea (S. Ulrich, Personal Communication, 1998). The samples from depths below 100 m do not consistently show anomalously high values of total bacterial numbers and biomass at the depth of the additional fluorescence maximum. However, the main features of the fluorescence characteristics as described above were

**Appendix 2** Profiles of (420/680) fluorescence from selected stations. See Appendix 1 for selection criteria



observed in the spectra taken with a LS50 luminescence spectrometer on both cruises (data not shown here).

#### 4.5 Deep red fluorescence observations in other regions

Red fluorescence at depths below the biologically productive upper water column has been reported for the Pacific Ocean since the early 1980s. Anderson (1982) observed a secondary fluorescence peak within a layer of

near-to-zero oxygen and nitrite concentrations. He suggested three possible mechanisms as being responsible for this effect: fluorescence from bacterial mitochondria, bacteriochlorophyll and microbial luminescence, but none of these hypotheses could be proved.

The most intensive study of red fluorescence maxima in deep waters was carried out by Broenkow et al. (1983, 1985, 1992) and Lewitus and Broenkow (1985). They reported on the presence of secondary and tertiary pigment maxima that were discussed in relation

to dissolved oxygen, the total attenuation coefficient and CTD data. The tertiary maximum appears to be a continuous feature of the OMZ of the North Pacific (Broenkow et al. 1992). The investigation of the spectral nature of this broad maximum led to several hypotheses of its origin. They concluded that dissolved sources can explain only parts, and found signs of a particulate nature of the fluorescence. Transport of fluorescent particles by marine snow and faecal pellets as well as lateral transport was proposed, while microbial decomposition may trigger the release of fluorophores. The fluorescence might be linked to senescent algae, cyanobacteria and non-chlorophyll pigments. A possible relationship between fluorescence and microbial biomass is stressed. The existence of a so far unknown heterotrophic bacterial population in the OMZ is suggested.

Some of these hypotheses are sustained by findings of Herbland (1978), Yentsch (1983) and Spinrad et al. (1989). Herbland (1978) studied "red soluble fluorescence" in the upper 150 m of the equatorial Atlantic Ocean. He observed a residual red fluorescence after filtration of samples using glass fibre filters. Its origin is thought to be the degradation or excretion of phytoplankton. Newer findings by Yentsch (1983) on the fluorescence characteristics of particles that pass through glass fibre filters indicate that, next to cyanobacteria, unknown very small phototrophic organisms pass the filters (pore size 0.45 µm). Red fluorescence was further reported for oxygen-deficient waters in coastal regions off Peru, by Spinrad et al. (1989) who proposed denitrifiers to be partly responsible for the observed *in situ* fluorescence, and Wishner et al. (1995), who report on a deep maximum of relative fluorescence, although less pronounced than in Broenkow and Lewitus (1985) or the data shown in this paper for the Arabian Sea.

## 5 Conclusions

While none of the considered hypotheses can be finally proven with the available information, the analysis of the data from the Arabian Sea presented in this paper leads to the following conclusions:

1. The fluorescence is more likely caused by the dissolved fraction, because the signal is detectable to the same extent in filtered and unfiltered samples.
2. The most intense signal is related to the top of the OMZ.
3. The fluorophore is destroyed within 1 year when stored refrigerated and in the dark, with no precautions taken to maintain anoxic conditions. It is, however, not degraded by a short-term presence of oxygen.
4. An absorption band at 420 nm is present in the spectra from samples of the OMZ. This "Gaussian part" of the absorption spectrum depicts the same vertical structure as the 660 nm fluorescence emission when excited at 420 nm.
5. It is likely that the absorption band at 420 nm and the fluorescence emission at 660 nm (when excited at 420 nm) belong together. This should be further investigated using excitation/emission spectroscopy.
6. There is no clear relationship between the enhanced red fluorescence intensity and the characteristic intermediate water masses of the Arabian Sea, although a dependence on water masses cannot be excluded. Instead, the enhanced red fluorescence seems to be a characteristic feature of depleted oxygen conditions, as they are found in the OMZ of the Arabian Sea.

**Acknowledgements** This work was supported by a grant from the Federal Minister of Education and Technology, Bonn, within the frame work of the JGOFS Arabian Sea program. We are grateful to the captain and the crew of RV *Somme* for their support. We are indebted to Mrs. Kirsten Neumann from the Institute of Marine Chemistry and Biogeochemistry of the University of Hamburg for providing the oxygen data, and to Mr. Nikolai Delling from the same institute for making the DOC and chlorophyll data available to us.

## References

- Anderson JJ (1982) The nitrite oxygen interface at the top of the oxygen minimum zone in the eastern tropical North Pacific. *Deep-Sea Res* 29: 1193–1201
- Barth H, Heuermann R, Loquay KD, Reuter R, Stute U (1997) Long-term stable sensors for bio-optical measurements. In: Stel JH, Behrens HWA, Borst JC, Droppert LJ and van der Meulen JP (eds) *Operational oceanography*, Elsevier Oceanography Series, Amsterdam, pp 133–140
- Breves W, Reuter R (2000) Bio-optical properties of gelbstoff in the Arabian Sea at the onset of the southwest monsoon. *Proc Ind Acad Sci EPS*, 109(4): 415–425
- Bricaud A, Morel A, Prieur L (1981) Absorption by dissolved organic matter (yellow substance) in the UV and visible domains. *Limnol Oceanogr* 26: 43–53
- Broenkow WW, Lewitus AJ, Yarbrough MA, Krenz RT (1983) Particle fluorescence and bioluminescence distributions in the eastern tropical Pacific. *Nature* 302: 329–331
- Broenkow WW, Lewitus AJ, Yarbrough MA (1985) Spectral observations of pigment fluorescence in intermediate depth waters of the North Pacific. *J Mar Res* 43: 875–891
- Broenkow WW, Yuen MA, Yarbrough MA (1992) VERTEX: biological implications of total attenuation and chlorophyll and phycoerythrin fluorescence distributions along a 2000-m-deep section in the Gulf of Alaska. *Deep-Sea Research* 39: 417–437
- Chen RF, Bada JL (1992) The fluorescence of dissolved organic matter in seawater. *Mar Chem* 37: 191–221
- Coble PG (1996) Characterization of marine and terrestrial DOM in seawater using excitation-emission matrix spectroscopy. *Mar Chem* 51: 325–346
- De Souza Sierra MM, Donard OFX (1991) Simulation of fluorescence variability in estuaries. *Oceanolog Acta* 11: 275–284
- Herbland A (1978) The soluble fluorescence in the open sea. *J Exp Mar Biol Ecol* 32: 275–284
- Heuermann R, Loquay KD, Reuter R (1995) A multi-wavelength *in situ* fluorometer for hydrographic measurements. *EARSeL Adv Remote Sensing* 3: 71–77
- Kalle K (1963) Über das Verhalten und die Herkunft der in den Gewässern und in der Atmosphäre vorhandenen himmelblauen Fluoreszenz. *D Hydrograph Z* 16: 153–166
- Kumar MD, Rajendran A, Somasundar K, Haake B, Jenisch A, Shuo Z, Ittekkot V, Desai BN (1990) Dynamics of dissolved organic carbon in the northwestern Indian Ocean. *Mar Chem* 31: 299–316

- Lal D (1994) Biogeochemistry of the Arabian Sea. Ind Acad Sci, Bangalore, pp 253
- Lewitus AJ, Broenkow WW (1985) Intermediate depth pigment maxima in oxygen minimum zones. *Deep-Sea Res* 32: 1101–1115
- Lorenzen CJ (1966) A method for the continuous measurement of in vivo chlorophyll concentration. *Deep-Sea Res* 13: 223–227
- Moran MA, Zepp RG (1997) Role of photoreactions in the formation of biologically labile compounds from dissolved organic matter. *Limnol and Oceanogr* 42: 1307–1316
- Naqvi WA (1991) Geographical extent of denitrification in the Arabian Sea in relation to some physical processes. *Oceanolog Acta* 14(3): 281–290
- Naqvi SWA (1994) Denitrification processes in the Arabian Sea. In: Lal D. (ed), *Biogeochemistry of the Arabian Sea*, Ind Acad of Sci, Bangalore, pp 181–202
- Naqvi SWA, Kumar MD, Narvekar PV, De Souza SN, George MD, D'Silva C (1993) An intermediate nepheloid layer associated with high microbial metabolic rates and denitrification in the northwest Indian Ocean. *J Geophys Res* 98: 16469–16479
- Nelson JR (1993) Detrital spectral absorption: Laboratory Studies of visible light effects on phytodetritus absorption, bacterial spectral signal, and comparison to field measurements. *J Mar Res* 51: 181–207
- Qasim SZ (1982): Oceanography of the northern Arabian Sea. *Deep-Sea Res* 29: 1041–1068
- Shetye SR, Gouveia AD, Shenoi SSC (1994) Circulation and water masses of the Arabian Sea. In: Lal D. (ed), *Biogeochemistry of the Arabian Sea*, Ind Acad Sci Bangalore, pp 9–26
- Shenoi SSC, Shetye SR, Gouveia AD, Michael GS (1993) Salinity extrema in the Arabian Sea. *SCOPE/UNEP Special Issue* 76: 37–49
- Spinrad RW, Glover H, Ward BB, Codispoti LA, Kullenberg G (1989) Suspended particle and bacterial maxima in Peruvian coastal waters during a cold water anomaly. *Deep-Sea Res* 36: 715–733
- Warren BA (1994) Context of the suboxic layer in the Arabian Sea. In: Lal D. (ed), *Biogeochemistry of the Arabian Sea*, Ind Acad Sci Bangalore, pp 203–216
- Wishner KF, Ashjian CJ, Gelfman C, Gowing MM, Kann L, Levin LA, Mullinfaux LS, Saltzman J (1995) Pelagic and benthic ecology of the lower interface of the Eastern Tropical Pacific oxygen minimum zone. *Deep-Sea Res* 42: 93–115
- Wishner KF, Gowing MM, Gelfman C (1998) Mesozooplankton biomass in the upper 1000 m in the Arabian Sea: overall seasonal and geographic patterns, and relationship to oxygen gradients. *Deep-Sea Res* 45: 2405–2433
- Yentsch CS (1983) A note on the fluorescence characteristics of particles that pass through glass-fiber filters. *Limnol Oceanogr* 28: 3, 597–599
- Yentsch CS, Menzel DW (1963) A method for the determination of phytoplankton chlorophyll and phaeophytin by fluorescence. *Deep-Sea Res* 10: 221–231
- You Y, Tomczak M (1993) Thermocline circulation and ventilation in the Indian Ocean derived from water-mass analysis. *Deep Sea Res I* 40: 13–56